Microchimica Acta (2020) 187:460
https://doi.org/10.1007/s00604-020-04449-7

ORIGINAL PAPER

Target-triggered configuration change of DNA tetrahedron for SERS assay of microRNA 122

Shufan Wang[1] · Caijun Wu[1] · Jiajia Luo[1] · Xiliang Luo[2] · Ruo Yuan[1] · Xia Yang[1]

Received: 29 September 2019 / Accepted: 11 July 2020

Abstract

A surface-enhanced Raman scattering (SERS) method is proposed for the assay of microRNA 122 based on configuration change of DNA tetrahedron. Firstly, a DNA tetrahedron was self-assembled with one vertex labeled with toluidine blue (TB). Then, it was immobilized on the porous Ni/SiO_2@PEI@Au as a SERS platform, which was characterized by scanning electron microscopy (SEM) and X-ray diffraction (XRD). At this time, the DNA tetrahedron was contracted; so, the TB is close to AuNPs and the Raman signal is high. When target microRNA 122 existed, with the nicking enzyme amplification strategy, a great deal of DNA signal chains (S5) was obtained, which can extend the contracted DNA tetrahedron and change it into a three-dimensional DNA tetrahedron. In this case, the TB was far from AuNPs, resulting in a lower Raman signal. Due to the configuration change of DNA tetrahedron, the Raman signal at 1624 cm^{-1} (with the excitation wavelength of 633 nm) has a linear relationship with the logarithm concentration of microRNA 122. This SERS assay has high sensitivity for microRNA 122 with a determination range from 0.01 aM to 10 fM and a detection limit of 0.009 aM. The recoveries from spiked samples were in the range 95 to 109%. This SERS strategy is designed based on the target-triggered configuration change of DNA tetrahedron, which can give new insight for DNA structures in bioanalysis.

Keywords SERS · microRNA 122 · DNA tetrahedron · Nicking enzyme amplification strategy

Introduction

MicroRNAs are small RNA molecules with the length of about 20 nucleotides (nt). They play crucial roles in both animals and plants in the development, fate, and death of cell by binding to the 3′-underslated region of messenger RNAs. [1, 2] Various microRNA expressions are directly related to numerous human diseases, like cancer, nervous system diseases, and cardiovascular; so, microRNAs become the key biomarkers to diagnose and prognose the cancer, [3] whereas the determination of microRNAs was an arduous task due to their limited size, susceptibility to degradation, low abundance, and sequence homology among family members (such as let-7 family of microRNA isoforms). [4, 5] Hence, we need to search for rapid, selective, and sensitive methods to detect microRNAs.

Nowadays, electrochemistry, [6] electrochemiluminescence, [7] microarray, [8] and fluorescence spectroscopy [9] have been used for assay of microRNA, but the detection limit needs to be improved. Surface-enhanced Raman spectroscopy (SERS) has become an excellent determination tool with the advantages of excellent nondestructive nature, [10] rapid response, less sample consumption, and superior specificity. [11, 12] Based on these properties, SERS has been rapidly developed and applied in many aspects, which can detect the trace levels of analysts such as microRNA. [13–16] SERS substrate is a key factor for SERS analysis. Noble metal nanoparticles such as Au and Ag are often

Electronic supplementary material The online version of this article (https://doi.org/10.1007/s00604-020-04449-7) contains supplementary material, which is available to authorized users.

✉ Ruo Yuan
yuanruo@swu.edu.cn

Xia Yang
xiayang2@swu.edu.cn

[1] Key Laboratory of Luminescence Analysis and Molecular Sensing (Southwest University), Ministry of Education, College of Chemistry and Chemical Engineering, Southwest University, Chongqing 400715, People's Republic of China

[2] Shandong Key Laboratory of Biochemical Analysis; College of Chemistry and Molecular Engineering, Qingdao University of Science and Technology, Qingdao 266042, People's Republic of China

Table 1 The nucleic acid sequence information

Name	Sequence(5′-3′)
microRNA 122 (Target)	UGG AGU GUG ACA AUG GUG UUU G
Assistant DNA	TAC TAG TGC GTG TCA CAC TCC A
Hairpin DNA	CAA ACA CCA TCG CAC TAG TAG CGG ATC GCT ACG GTG TCC GCA GT
S1	HOOC-ACA TTC CTA AGT CTG AAT TCC TGG AGA TAC ATG GCA TTA TTA CAG CTT GCT ACA CGC CCT ATT AGA AGG TCC GAT TGA AGA GCC GTA G
S2	NH_2-$(CH_2)_6$-TAT CAG CAG GCA GTT GAC GCG ACA GTC GTT CAA GCC TTT CGG ACC TTC TAA TAG GGC GTG TAG CAA GCT GTA ATT TAT GCG AGG GTC CAA TAC TCT GTT CCG GGT GTG GCA T
S3	NH_2-$(CH_2)_6$-GGC TTG AAC GAC TGT CGC GTC AAC TGC CTG CTG ATA TTA CGA CAC TAC GTA ACG GTC GAG GAC TGC TCC GCT GAT TAC TGC GGA CAC CGT AGC GAT CCG CCT ACG GCT CTT C
S4	NH_2-$(CH_2)_6$-TGC CAT GTA TCT CCA GGA ATT CAG ACT TAG GAA TGT TTT CAG CGG AGC AGT CCT CGA CCG TTA CGT AGT GTC GTT TAT GCC ACA CCC GGA ACA GAG TAT TGG ACC CTC GCA T
microRNA 21	UAG CUU AUC AGA CUG AUG UUG A
microRNA 126	CAU UAU UAC UUU UGG UAC
microRNA let7a	UGA GGU AGU AGG UUG UAU AGU U

used as the enhancement substrate. But the disadvantage is that the nanoparticles are easy to aggregate and not uniform. Using the magnetic Ni to concentrate the Au nanoparticles and enhance the Raman signal is one efficient method. So, in this work, Ni/SiO_2@PEI@AuNPs was employed as the SERS substrate.

DNA nanostructures have been applied in various biomedical fields due to the prominent programming properties, high precision, and outstanding controllability. [17] Zhang et al. designed a highly ordered 3D DNA nanomachine for rapid determination of microRNA. [18] Zhu et al. designed DNA walkers-triggered fluorescence spots as self-built compartments to quantify the nucleic acid. [19] DNA tetrahedron is an excellent nanoarchitecture due to their merits of three-dimensional scaffold structural stability, specific orientation, which are utilized for biomolecular probe carrier, [20] electrochemical switching, [21] photoelectrochemical biosensor, [22], and so on.

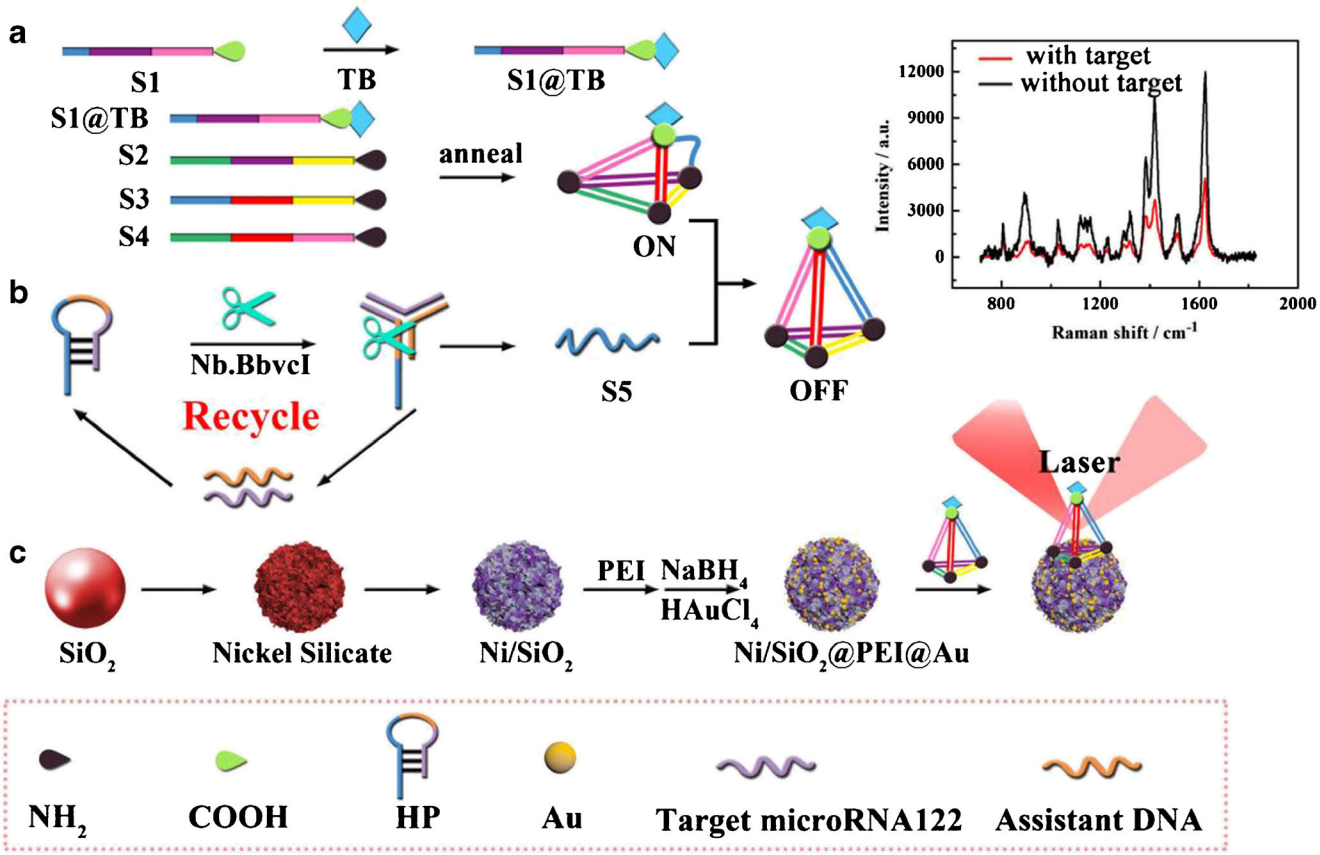

Scheme 1 The diagram for preparation of SERS method

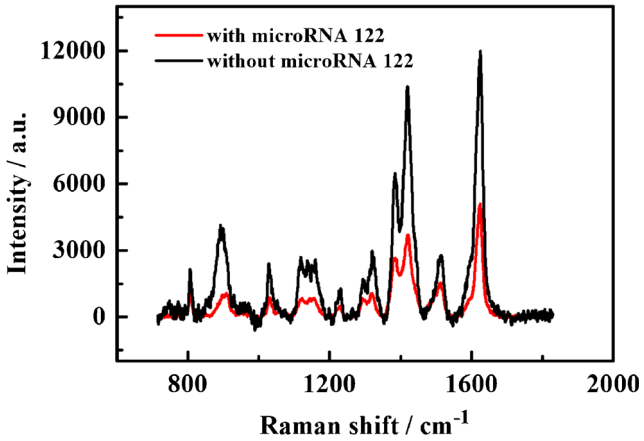

Fig. 1 SERS of the platform with target microRNA 122 (red curve) and without microRNA 122 (black curve)

In this work, a SERS method is fabricated to detect microRNA 122 by employing configuration change of DNA tetrahedron. The SERS strategy has low detection limit and good selectivity to detect microRNA 122, which may be applied for analysis of proteins, microRNA, etc.

Experimental section

Nicking enzymes mediated signal amplification

A total of 10 μL of hairpin DNA (1 μM), assistant DNA (1 μM), and various concentrations of the target microRNA 122 were mixed under shaking. Then, 8 U of Nb.BbvC*I* nicking enzyme in 10 × NE buffer was dropped into above solution and incubated for 65 min at 37 °C to obtain enough sequences of S5. To terminate the reaction, the mixtures were kept at 80 °C for 20 min [23]. Then, the products were cooled naturally.

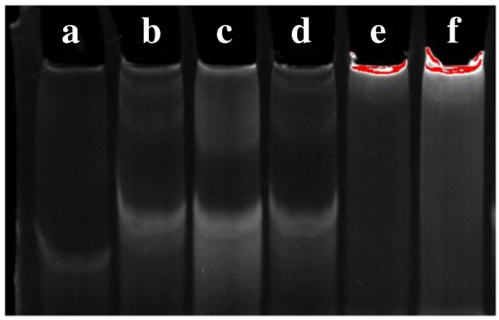

Fig. 3 PAGE analysis of the DNA structure. **a**–**e** The DNA S1, S2, S3, S4, the contracted DNA tetrahedron, and the structure after S5 added into the contracted DNA tetrahedron

Fabrication of the SERS method

The *Ni/SiO$_2$@PEI@AuNPs* and DNA tetrahedron are shown in the supporting information and the sequences of nucleotide are listed in Table 1. The above DNA tetrahedron S4/S3/S2/S1@TB was mixed with the sequences of S5. The mixture was incubated at room temperature for 110 min to obtain the extended DNA tetrahedron. To obtain the SERS signal, 30 μL of Ni/SiO$_2$@PEI@AuNPs was dropped into the solution of extended DNA tetrahedron under shaking for 12 h at 4 °C. Then, 10 μL of extended DNA tetrahedron@Ni/SiO$_2$@PEI@AuNPs was dropped onto silicon wafer and dried before the SERS measurement. Finally, the platform

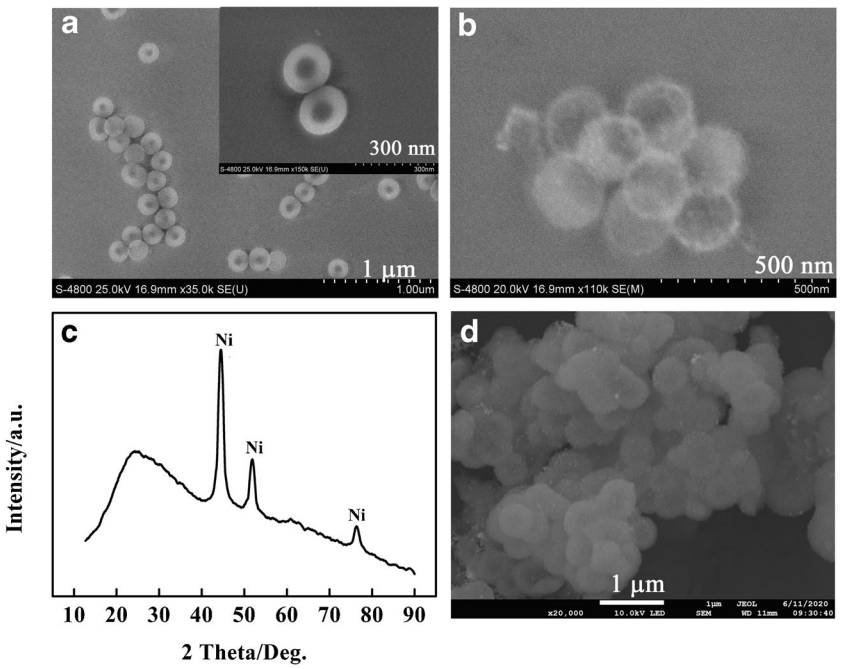

Fig. 2 SEM of **A** SiO$_2$ (inset: enlarged image), **B** Ni/SiO$_2$, **D** Ni/SiO$_2$@PEI@AuNPs, **C** XRD of Ni/SiO$_2$

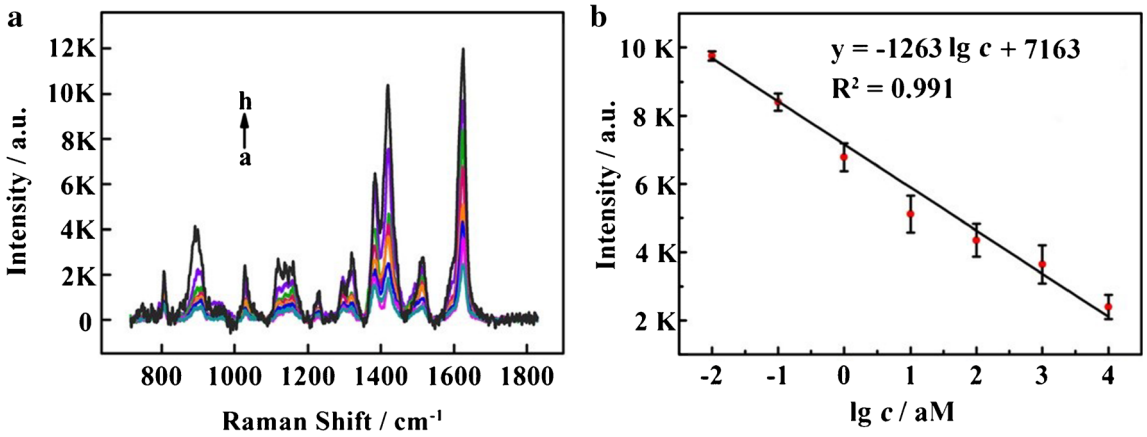

Fig. 4 **A** SERS responses of the proposed method with a series of concentrations (0.01 aM to 10 fM, from g to a, h: 0 aM) of microRNA 122. **B** Calibration plot of SERS peak current versus the logarithm of microRNA 122 concentration (without curve h). Error bars: SD, $n = 3$

was measured by Raman microscope (Renishaw Invia Raman spectrometer, Invia, UK) with the excitation wavelength of 633 nm.

Results and discussion

Principle of SERS platform

Scheme 1 shows the fabrication process of the SERS method. Firstly, Ni/SiO_2@PEI@AuNPs was employed as the SERS platform. The porous Ni/SiO_2 was used as support to absorb more AuNPs and DNA tetrahedron. Secondly, four DNA single strands self-assembled a contracted DNA tetrahedron with one vertex labeled with toluidine blue (TB), which was immobilized on the Ni/SiO_2@PEI@AuNPs. Then, a cycle enzyme amplification strategy was induced by target microRNA 122 to obtain a large number of S5 chains. When the microRNA 122 was absent, a high Raman signal was obtained because TB was near to the AuNPs. When the microRNA existed, a large amount of S5 was obtained and the contracted DNA tetrahedron was extended and turned into a three-dimensional DNA tetrahedron, leading to the toluidine blue far from AuNPs. With the increasing amount of microRNA 122, the configuration of contracted DNA tetrahedron changed a lot and formed more extended DNA tetrahedron to decrease the Raman signal. Therefore, the signal was negatively linearly correlated with the concentration of microRNA 122. When the microRNA 122 was absent (Fig. 1, black curve), a high Raman signal was achieved. With the adding of microRNA 122 (the concentration was 10 aM), S5 chain can be obtained and the configuration of contracted DNA tetrahedron changed resulting in the Raman signal decrease (Fig. 1, red curve). And the peak at 1624 cm^{-1} was selected as the detecting standard of the microRNA 122.

Characterization of materials

Figure 2 A shows the scanning electron microscopy (SEM) of SiO_2, which is hollow ball-shaped with average size of about 200 nm. Figure 2 B is the SEM of Ni/SiO_2, which also showed porous sphere morphology. As displayed in Fig. 2C, the X-ray diffraction (XRD) of Ni/SiO_2 matches with the JCPDS file no.04-0850. The peak at 44.5°, 51.8°, and 76.3° is indexed to the (111), (200), and (220) crystal plane of Ni. And the peak at about 25° was corresponding to SiO_2. [24] Figure 2 D is the SEM image of Ni/SiO_2@Au, in which we can find that the AuNPs were adhered to the surface of Ni/SiO_2.

Table 2 Performance of the proposed method compared with other methods for determination of microRNA 122

Analytical method	Target	LOD	Linear range	Refs
Fluorescence	microRNA 122	6 pM	250 pM to 4 nM	[27]
Photoelectrochemistry (PEC)	microRNA 122	83 fM	100 fM to 3 nM	[28]
Surface plasmon resonance (SPR)	microRNA 122	50 aM	50 aM to 10 pM	[29]
Electrochemiluminescence (ECL)	microRNA 122	3 aM	0.01 fM to 10 pM	[30]
Square wave voltammetry (SWV)	microRNA 122	32 aM	10 aM to 50 fM	[31]
SERS	microRNA 122	7.75 aM	10 aM to 100 pM	[32]
SERS	microRNA 122	0.009 aM	0.01 aM to 10 fM	This work

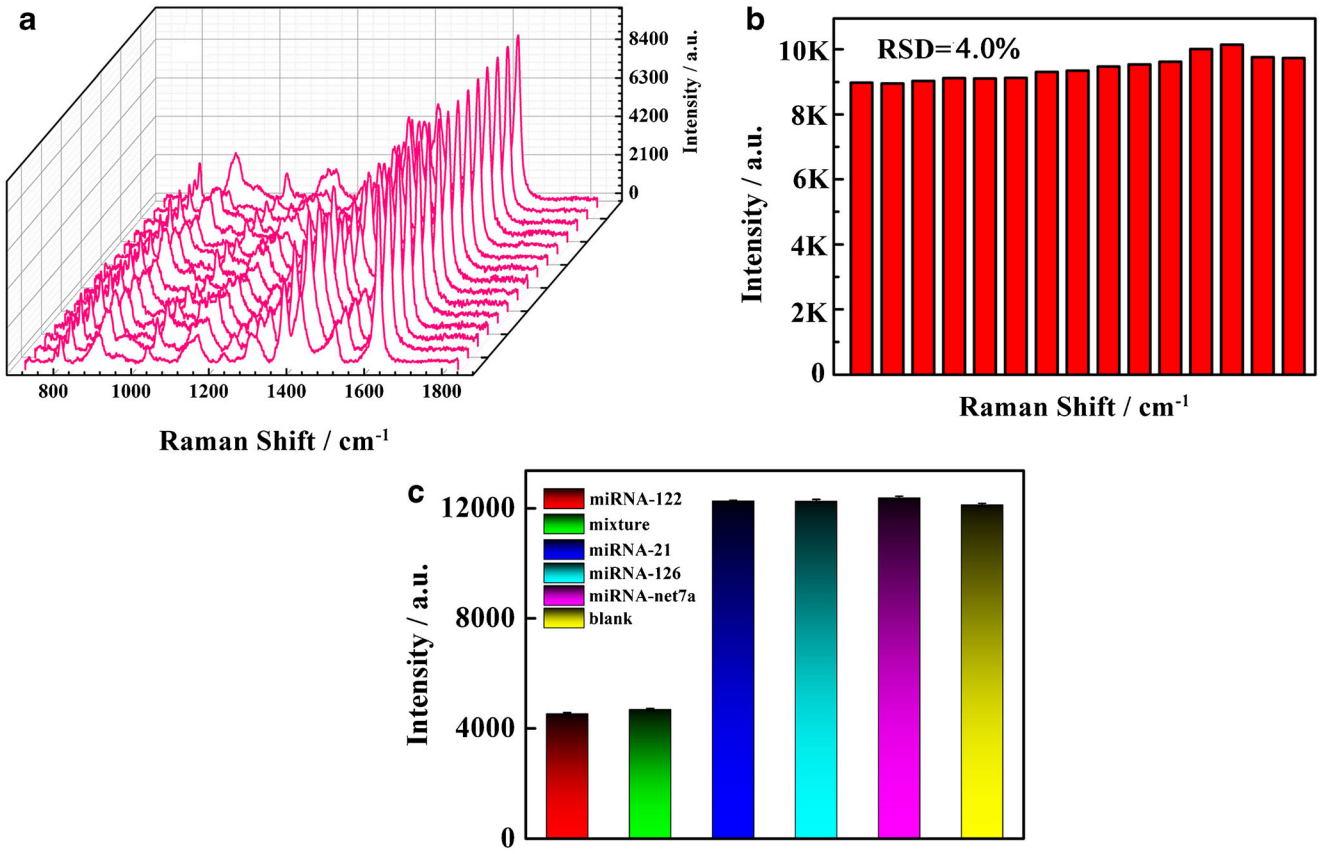

Fig. 5 **A** SERS assay acquired at 15 different spots, **B** RSD of the Raman intensity at 1624 cm^{-1} for 15 spots, and **C** SERS response with various interference agents

Optimization of experimental conditions

The following parameters were optimized: (a) the circle time of Nb.BbvC*I*. and (b) the incubation time of intermediate sequences of S5. Respective text and figures on optimizations are given in the Electronic Supporting Material (Fig. S1). In short, the following experimental conditions were found to give best results: (a) the best circle time of Nb.BbvC*I*. was 60 min and (b) 110 min was chosen as the incubation time of intermediate sequences of S5.

The polyacrylamide gel electrophoresis test

We employed polyacrylamide gel electrophoresis (PAGE) to see whether the DNA structure formed (Fig. 3). Lanes a–e represented the DNA S1, S2, S3, S4, the contracted DNA tetrahedron, and the structure after S5 added into the contracted DNA tetrahedron. After annealing the four DNA strands, a band with low mobility was observed (lane e), illustrating the formation of a DNA tetrahedron. Then, after the process of target induced the nicking enzyme-mediated signal amplification, S5 was obtained. And when S5 was added into the contracted DNA tetrahedron (lane f), it also showed a low mobility, which has no obvious difference with lane e. The reason is that although the contracted DNA tetrahedron was extended, the structure was large and cannot move quickly.

Determination *property of the proposed method*

Target microRNA 122 was used to evaluate the performance of the proposed method on the condition that it was under the ideal experimental conditions. Figure 4 shows the

Table 3 Determination of microRNA 122 in human serum ($n = 3$)

Serum number	Added concentration/aM	Found concentration/aM	Recovery /%	RSD/%
1	1	1.09	109	0.13
2	10	9.5	95	1.82
3	100	96.4	96.4	0.85
4	1000	980	98	0.47
5	10,000	9960	99.6	1.39

relationships of the Raman intensity for the microRNA 122 with a series concentrations ranging from 0.01 aM to 10 fM and the linear property of the assay. Figure 4 A and B revealed that the Raman intensity at 1624 cm^{-1} diminished gradually with the increasing amount of microRNA 122. And when no microRNA 122 existed, the highest peak appears (curve h in Fig. 4A). From Fig. 4B, the plot of the Raman signal at 1624 cm^{-1} versus the logarithm of the microRNA 122, possessed excellent linearity between 0.01 aM and 10 fM with the linear function of $y = -1263\ \lg c + 7163$ ($R^2 = 0.991$). According to the IUPAC method [25, 26], the detection limit (LOD) of microRNA 122 was figured as 0.009 aM (S/N = 3). Each concentration of microRNA 122 was tested three times to calculate the error bar. Contradistinguished with other method for the determination of microRNA 122 (Table 2), this SERS method exhibited good performance.

Reproducibility

The reproducibility of the SERS method is critical to its practical application. Fifteen different spots in one silicon wafer were chosen to verify the reproducibility of this SERS assay. As displayed in Fig. 5A, it is similar among these 15 spots. From Fig. 5B, the relative standard deviation (RSD) of the peak is 4.0%, which demonstrates the excellent reproducibility of this method.

Selectivity

The selectivity of the SERS method was examined by using other microRNAs, including microRNA 21 (10 fM), microRNA 126 (10 fM), microRNA let7a (10 fM), and the blank solution without any microRNA. Besides, the mixed analytical solution containing 0.1 fM of target microRNA 122 is also tested by this method, which exhibits a same SERS signal as that only with microRNA 122 (Fig. 5C). This result proves the high specificity of the SERS platform.

Preliminary application

To verify the applicability of the fabricated SERS method for real samples, the experiment of the SERS strategy was conducted by detecting microRNA 122 in 100-fold diluted healthy human serum samples (obtained from Xinqiao Hospital of Army Medical University). The experimental details were given in the supporting information. Different concentrations of microRNA 122 were added into the diluted healthy human serum and the proposed method was employed to detect the value of microRNA by using the obtained calibration plot. The recovery was calculated by the found concentration/added concentration. From Table 3, the recoveries are 109%, 95%, 96.4%, 98%, and 99.6%. And the RSD values are from 0.13% to 1.82%, which is acceptable for quantitative methods in clinical determination of microRNA 122. The major disadvantage of the proposed method is the reversibility, which is the orientation of our future study.

Conclusions

In this work, we designed a SERS method employing the configuration change of DNA tetrahedron for determination of target microRNA 122. The microRNA 122 induce the cycle enzyme amplification strategy and a large number of S5 chains can be obtained, which can extend the contracted DNA tetrahedron. This would lead to the TB far from AuNPs, resulting in a lower Raman signal. This method has good sensitivity and excellent selectivity. This SERS strategy is smartly designed by the configuration change of DNA tetrahedron to indirectly control the position of TB and hot spot, which can be utilized in potential applications for other biomolecular analysis.

Acknowledgments This work was supported by the Chongqing Research Program of Basic Research and Frontier Technology (cstc2019jcyj-msxmX0209), Fundamental Research Funds for the Central Universities (XDJK2019C077), Open Project Program of College of Chemistry and Molecular Engineering, Qingdao University of Science and Technology (QUSTHX201804).

Funding information The authors also thank Xia Zhong (Southwest University) for the Raman test technical support.

Compliance with ethical standards

Conflict of interest The authors declare that they have no conflict of interest.

References

1. Bartel DP (2018) Metazoan microRNAs. Cell 173:20–51
2. Li J, Li DX, Yuan R, Xiang Y (2017) Biodegradable MnO_2 nanosheet-mediated signal amplification in living cells enables sensitive detection of down-regulated intracellular microRNA. ACS Appl Mater Interfaces 7:5717–5724
3. Wang MQ, Yu Y, Liu FN, Ren L, Zhang QJ, Zou G (2018) Single polydiacetylene microtube waveguide platform for discriminating MicroRNA-215 expression levels in clinical gastric cancerous, paracancerous and normal tissues. Talanta 188:27–34
4. Kilic T, Erdem A, Ozsoz M, Carrara S (2018) microRNA biosensors: opportunities and challenges among conventional and commercially available techniques. Biosens Bioelectron 99:525–546
5. Shabaninejad Z, Yousefi F, Movahedpour A, Ghasemi Y, Dokanehiifard S, Rezaei S, Aryan R, Savardashtaki A, Mirzaei H (2019) Electrochemical-based biosensors for microRNA detection: nanotechnology comes into view. Anal Biochem 581:113349
6. Miao P, Zhang T, Xu JH, Tang YG (2018) Electrochemical detection of microRNA combining T7 exonuclease-assisted cascade

signal amplification and DNA-templated copper nanoparticles. Anal Chem 90:11154–11160
7. Peng LC, Yuan YL, Fu XM, Fu A, Zhang P, Chai YQ, Gan XX, Yuan R (2019) Reversible and distance-controllable DNA scissor: a regenerated electrochemiluminescence biosensing platform for ultrasensitive detection of microRNA. Anal Chem 91:3239–3245
8. Sun XL, Wang H, Jian YN, Lan FF, Zhang LN, Liu HY, Ge SG, Yu JH (2018) Ultrasensitive microfluidic paper-based electrochemical/visual biosensor based on spherical-like cerium dioxide catalyst for miR-21 detection. Biosens Bioelectron 105:218–225
9. He MQ, Wang K, Wang WJ, Yu YL, Wang JH (2017) Smart DNA machine for carcinoembryonic antigen detection by exonuclease III-assisted target recycling and DNA walker cascade amplification. Anal Chem 2017(89):9292–9298
10. Browne WR, McGarvey JJ (2007) The Raman effect and its application to electronic spectroscopies in metal-centered species: techniques and investigations in ground and excited states. Coord Chem Rev 2007(251):454–473
11. Huang ZP, Zhang R, Chen H, Weng WH, Lin QY, Deng D, Li Z, Kong JL (2019) Sensitive polydopamine bi-functionalized SERS immunoassay for microalbuminuria detection. Biosens Bioelectron 142:111542
12. Dong H, Yao DZ, Zhou Q, Zhang LM, Tian Y (2019) An integrated platform for the capture of circulating tumor cells and in situ SERS profiling of membrane proteins through rational spatial organization of multi-functional cyclic RGD nanopatterns. Chem Commun 55:1730–1733
13. Miao XR, Wen SP, Su Y, Fu JJ, Luo XJ, Wu P, Cai CX, Jelinek R, Jiang LP, Zhu JJ (2019) Graphene quantum dots wrapped gold nanoparticles with integrated enhancement mechanisms as sensitive and homogeneous substrates for surface-enhanced Raman spectroscopy. Anal Chem 91:7295–7303
14. Tian HH, Li HB, Fang Y (2019) Binary thiol-capped gold nanoparticle monolayer films for quantitative surface-enhanced Raman scattering analysis. ACS Appl Mater Interfaces 11:16207–16213
15. Lee JU, Kim WH, Lee HS, Park KH, Sim SJ (2019) Quantitative and specific detection of exosomal microRNAs for accurate diagnosis of breast cancer using a surface-enhanced Raman scattering sensor based on plasmonic head-flocked gold nanopillars. Small 15:1804968
16. Jiang N, Hu Y, Wei W, Zhu T, Yang K, Zhu G, Yu M (2019) Detection of microRNA using a polydopamine mediated bimetallic SERS substrate and a re-circulated enzymatic amplification system. Microchim Acta 186:65
17. Suo ZG, Chen JQ, Hou XL, Hu ZH, Xing FF, Feng LY (2019) Growing prospects of DNA nanomaterials in novel biomedical applications. RSC Adv 9:16478–16491
18. Zhang P, Jiang J, Yuan R, Zhuo Y, Chai YQ (2018) Highly ordered and field-free 3D DNA nanostructure: the next generation of DNA nanomachine for rapid single-step sensing. J Am Chem Soc 140: 9361–9364
19. Zhu LY, Liu QH, Yang BY, Ju HX, Lei JP (2018) Pixel counting of fluorescence spots triggered by DNA walkers for ultrasensitive quantification of nucleic acid. Anal Chem 90:6357–6361
20. Lin Y, Jia JP, Yang R, Chen DZ, Wang J, Luo F, Guo LH, Qiu B, Lin ZY (2019) Ratiometric immunosensor for GP73 detection based on the ratios of electrochemiluminescence and electrochemical signal using DNA tetrahedral nanostructure as the carrier of stable reference signal. Anal Chem 91:3717–3724
21. Wang D, Chai YQ, YuanYL YR (2019) Precise regulation of enzyme cascade catalytic efficiency with DNA tetrahedron as scaffold for ultrasensitive electrochemical detection of DNA. Anal Chem 91:3561–3566
22. Li MJ, Xiong CY, Zheng YN, Liang WB, Yuan R, Chai YQ (2018) Tetrahedron as nanocarrier for efficient immobilization of CdTe QDs-methylene blue as signal probe with near-zero background noise. Anal Chem 90:8211–8216
23. Liu Q, Ma C, Liu XP, Wei YP, Mao CJ, Zhu JJ (2017) A novel electrochemiluminescence biosensor for the detection of microRNAs based on a DNA functionalized nitrogen doped carbon quantum dots as signal enhancers. Biosens Bioelectron 92:273–279
24. Tang C, Liu Y, Chang X, Zhu J, Wei X, Zhou L, He L, Yang W, Mai LQ (2017) Ultrafine nickel-nanoparticle-enabled SiO_2 hierarchical hollow spheres for high-performance lithium storage. Adv Funct Mater 28:1704561
25. International Union of Pure and Applied Chemistry (1976) Analytical chemistry division. Pure Appl Chem 45:105–123
26. Long GL, Winefordner JD (1983) Limit of detection. A closer look at the IUPAC definition. Anal Chem 55:712A–724A
27. Liu MX, Liang SP, Tang YF, Tian JN, Zhao YC, Zhao SL (2018) Rapid and label-free fluorescence bioassay for microRNA based on exonuclease III-assisted cycle amplification. RSC Adv 8:15967–15972
28. Liu SS, Cao HJ, Wang XY, Tu WW, Dai ZH (2018) Green light excited ultrasensitive photoelectrochemical biosensing for microRNA at a low applied potential based on the dual role of Au NPs in TiO_2 nanorods/Au NPs composites. Nanoscale 10:16474–16478
29. Gu Y, Song J, Li MX, Zhang TT, Zhao W, Xu JJ, Liu ML, Chen HY (2017) Ultrasensitive microRNA assay via surface plasmon resonance responses of Au@Ag nanorods etching. Anal Chem 89:10585–10591
30. Li YL, Yu C, Yang B, Liu ZR, Xia PY, Wang Q (2018) Target-catalyzed hairpin assembly and metal-organic frameworks mediated nonenzymatic co-reaction for multiple signal amplification detection of MiR-122 in human serum. Biosens Bioelectron 102:307–315
31. Miao P, Jiang YT, Zhang T, Huang Y, Tang YG (2018) Electrochemical sensing of attomolar microRNA combining cascade strand displacement polymerization and reductant-mediated amplification. Chem Commun 54:7366–7369
32. He Y, Yang X, Yuan R, Chai YQ (2019) A novel ratiometric SERS biosensor with one Raman probe for ultrasensitive microRNA detection based on DNA hydrogel amplification. J Mater Chem B 7: 2643–2647